

Cite this: DOI: 10.1039/c0xx00000x

www.rsc.org/xxxxxx

ARTICLE TYPE

## Tuning of gallery heights in a crystalline 2D carbon nitride network

Samantha Y. Chong,<sup>a</sup> James T. A. Jones,<sup>a</sup> Yaroslav Z. Khimyak,<sup>b</sup> Andrew I. Cooper,<sup>a</sup> Arne Thomas,<sup>c</sup> Markus Antonietti,<sup>d</sup> and Michael J. Bojdys<sup>\*a</sup>

Received (in XXX, XXX) Xth XXXXXXXXX 20XX, Accepted Xth XXXXXXXXX 20XX

DOI: 10.1039/b000000x

Poly(triazine imide) – a 2D layered network – can be obtained as an intercalation compound with halides from the ionothermal condensation of dicyandiamide in a eutectic salt melt. The gallery height of the intercalated material can be tuned via the composition of the eutectic melt and post-synthetic modification. Herein, we report the synthesis of poly(triazine imide) with intercalated bromide ions (PTI/Br) from a lithium bromide and potassium bromide salt melt. PTI/Br has a hexagonal unit-cell ( $P6_3cm$  (no. 185);  $a = 8.500390(68)$  Å,  $c = 7.04483(17)$  Å) which contains two layers of imide-bridged triazine ( $C_3N_3$ ) units stacked in an AB-fashion as corroborated by solid-state NMR, FTIR spectroscopy and high-resolution TEM. Contrasted with a recently reported, analogous PTI/Li<sup>+</sup>Cl<sup>-</sup> from a LiCl/KCl eutectic, the layer-stacking distance was expanded from 3.38 Å to 3.52 Å going from chloride to bromide, respectively, – an exceptionally large spacing for aromatic, discotic systems (c.f. graphite with 3.35 Å). Subsequent treatment of PTI/Br with concentrated ammonium fluoride yields poly(triazine imide) with intercalated fluoride ions (PTI/F) ( $P6_3/m$  (no. 176);  $a = 8.4212(4)$  Å,  $c = 6.6381(5)$  Å) as a statistical phase mix with PTI/Br. Fluoride intercalation leads to a contraction of the gallery height to 3.32 Å.

### Introduction

The quest for carbon nitrides – in particular their saturated, sp<sup>3</sup>-hybridised, crystalline allotropes – has remained topical for the last decades, as theory predicts exceptional mechanical properties for this class of materials.<sup>1-3</sup> This research area has gained momentum in recent years from a different direction: the layered graphitic (C, N) materials which are not only deemed to be potential precursors for the predicted high-density sp<sup>3</sup>-bonded phases,<sup>4-6</sup> but show interesting properties in their own right, such as metal-free catalytic and photocatalytic activity.<sup>3, 7-11</sup> Realisation of such two-dimensional, covalently bonded molecular sheets with a periodic structures is a fascinating and challenging research target in its own right,<sup>12</sup> as seen for example in graphene research and the recent development of 2D covalent frameworks.<sup>13-16</sup>

Previous attempts at bulk synthesis of carbon nitrides faltered on account of e.g. incomplete condensation or polymerisation of molecular precursors yielding non-stoichiometric, amorphous solids in most cases – as was critically appraised in later years.<sup>17-20</sup> Sundermeyer et al. performed organic chemistry in molten salts already in the 1960s, pointing out the good solvating properties of the eutectic mixture of LiCl and KCl with respect to nitrides, carbides, cyanides, cyanates and thiocyanates,<sup>21, 22</sup> and inorganic salt melts have been utilised for the synthesis of extended, covalently bonded, organic frameworks.<sup>15, 23-26</sup> The use of eutectic salt melts as solvent and structure-directing agent in the polycondensation and deamination reaction of dicyandiamide recently lead to the successful synthesis of poly(triazine imide)

with intercalated lithium and chloride ions (PTI/Li<sup>+</sup>Cl<sup>-</sup>) with a remarkably low content of hydrogen, and a previously unequalled crystallinity.<sup>27, 28</sup> PTI/Li<sup>+</sup>Cl<sup>-</sup> consists of extended 2D layers of covalently linked triazine ( $C_3N_3$ ) units with a delocalized  $\pi$ -electron system via imide-bridges. The apparent structural analogy to graphite extends to the accessibility of interlayer space to guest molecules. In the case of PTI/Li<sup>+</sup>Cl<sup>-</sup>, chloride ions are found in the interstitial space between layers while Li<sup>+</sup> ions decorate the trigonal voids spanned by neighbouring triazine units (c.f. Fig. 1, A).

Herein we report, that the gallery height of this layered graphitic (C, N) material can be tuned by the choice of the intercalated halide. Lithium bromide and potassium bromide eutectic employed in analogous fashion for the preparation of poly(triazine imide) yields a layered stage I intercalation compound with full substitution of chloride by bromide. Subsequent treatment of PTI/Br with concentrated ammonium fluoride distorts the inter-layer ordering and causes statistical replacement of bromide by fluoride anions. The exchange of guest anions is accompanied by expansion or deflation of stacking distances as a function of their ionic radii. Furthermore, swelling of PTI/halide galleries opens up a potential way for the exfoliation of this interesting 2D material.

### Experimental

#### Synthesis of PTI/Br

Lithium bromide and potassium bromide eutectic (LiBr/KBr, 52:48 wt %, m.p. 348 °C) was prepared according to literature.<sup>29</sup> Dicyandiamide (2 g, 23.79 mmol) was thoroughly ground with

10 g of LiBr/KBr. The reaction mixture was heated at 40 K min<sup>-1</sup> under inert atmosphere and kept at the terminal temperature of 600 °C for 48 h. After natural cooling, excess salt was removed in boiling distilled water. The product was thoroughly dried at 200 °C under vacuum to yield PTI/Br (1.16 g, 6.29 mmol, 79 % yield) as a yellow-brown powder.

### Synthesis of PTI/F

Poly(triazine imide) with intercalated bromide ions (PTI/Br) (200 mg, 1.08 mmol) was stirred and heated at 60 °C for 48 h in aqueous ammonium fluoride solution (100 mL, 8 M). The solid was filtered off and washed repeatedly with distilled water. The yellow-brown powder was thoroughly dried at 200 °C under vacuum to yield a statistical mix of PTI/F and PTI/Br (42 mg, 0.67 mmol, 62 % yield).

### Results and Discussion

Elemental microanalysis and ICP of PTI/Br gave the following values: C, 32.6; N, 56.4; H, 0.97; O, 4.7; Br, 3.82; and Li, 1.51 wt %. An approximate composition of the material is C<sub>12</sub>N<sub>17.8</sub>H<sub>4.3</sub>Br<sub>0.2</sub>Li<sub>1.0</sub>, which is comparable with PTI/Li<sup>+</sup>Cl<sup>-</sup> and C<sub>6</sub>N<sub>9</sub>H<sub>3</sub>·HCl, if somewhat deficient in bromide, lithium and nitrogen. This is in parts due to inhomogeneous distribution of halides and introduction of vacancies in the interstitial space brought on by the washing procedure.

ATR-FTIR spectroscopy of the material shows fairly broad features characteristic of a network (Fig. 1). The region from 1200 to 1600 cm<sup>-1</sup> can be assigned to stretching modes of (C, N) heterocycles, and the sharp feature at 805 cm<sup>-1</sup> is classically attributed to the out-of-plane breathing mode of triazine (C<sub>3</sub>N<sub>3</sub>) units. Peaks at 3300 and 3180 cm<sup>-1</sup> indicative of secondary and primary amines (and their intermolecular H-bonding) can be discerned, which is in agreement with the results from elemental analysis.

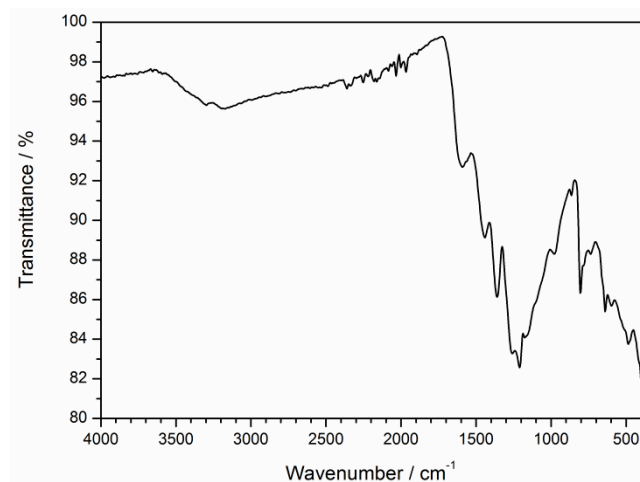


Fig. 1 ATR-FTIR spectrum of PTI/Br showing characteristic N-H stretches at 3300 and 3180 cm<sup>-1</sup> as well as the breathing-mode of the triazine (C<sub>3</sub>N<sub>3</sub>) unit at 805 cm<sup>-1</sup>.

Quantitative solid-state <sup>13</sup>C{<sup>1</sup>H} magic-angle-spinning (MAS) NMR data of PTI/Br shows three features at 168.5, 163.3 and 158.2 ppm which are in broad agreement with the carbon environments found for PTI/Li<sup>+</sup>Cl<sup>-</sup> (Fig. 2, A). From <sup>13</sup>C cross-polarization (CP)/MAS NMR data can be seen that the resonance

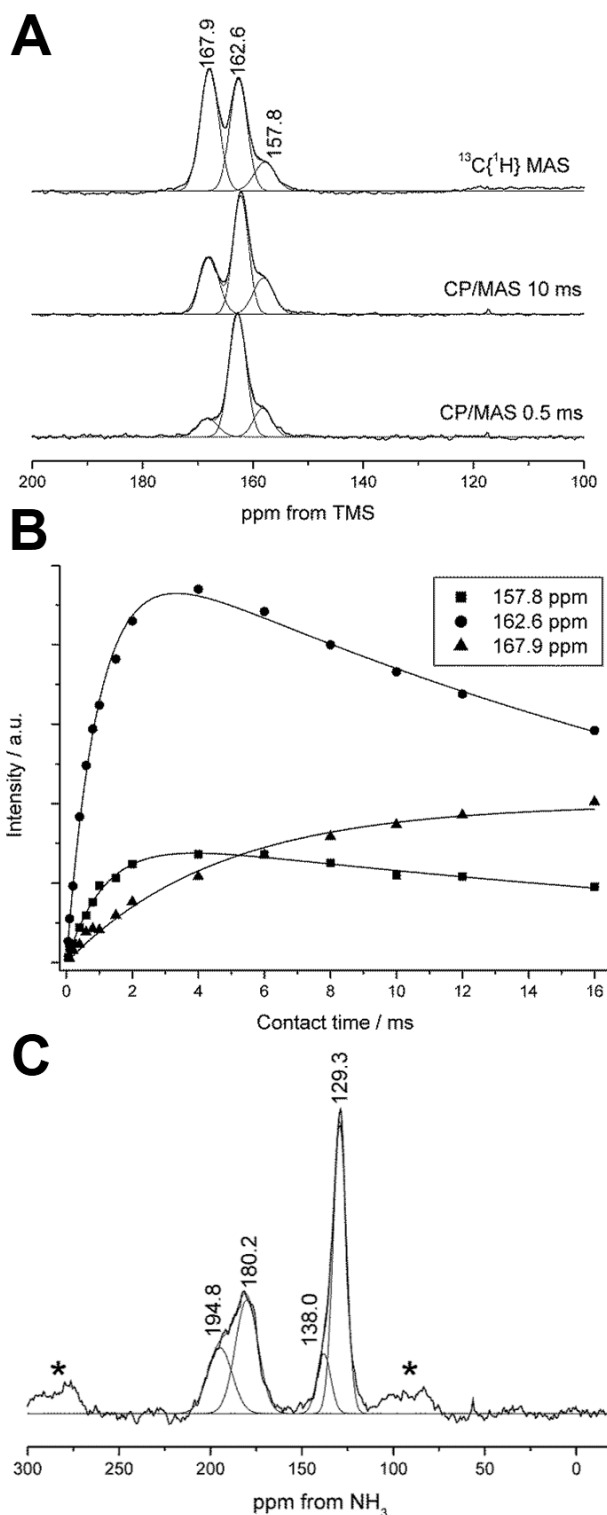
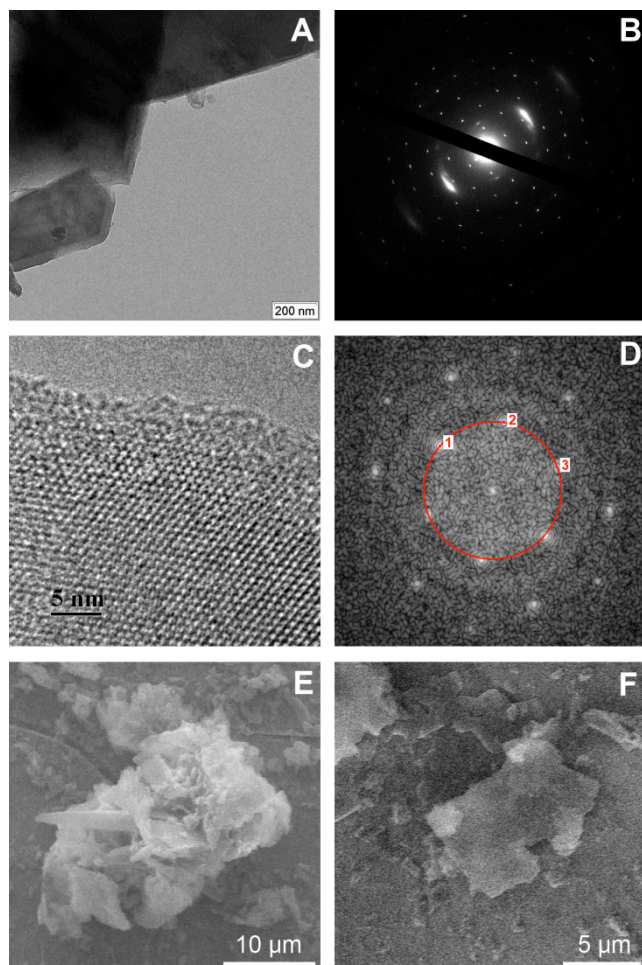


Fig. 2 Solid-state NMR investigation of PTI/Br showing <sup>13</sup>C{<sup>1</sup>H} MAS and <sup>13</sup>C CP/MAS NMR spectra (A), <sup>13</sup>C CP/MAS NMR kinetics curves (B), and a <sup>1</sup>H-<sup>15</sup>N CP/MAS NMR spectrum (τ = 5 ms) (C). Spinning sidebands are denoted with asterisks.

at 168.5 ppm displays very long CP build-up kinetics and shows no evidence of relaxation in the rotating frame, which is typical for a carbon environment with very few protons in its proximity (c.f. Table S1, ESI). Hence, this signal can be assigned to the

carbons in the triazine ring. The two resonances at 163.3 and 158.2 ppm show CP



**Fig. 3** Representative TEM image of PTI/Br showing sharp breaking edges with characteristic 120° and 60° angles (A), and corresponding SAED pattern (B). The hexagonal pattern in the  $hk0$  plane corresponds to a lattice constant of  $a = 8.50 \text{ \AA}$  and the smeared out reflexes along the  $00l$  direction correspond to  $c = 7.04 \text{ \AA}$ . HRTEM image (C), and corresponding Fourier transform image (D); the red circle indicates a distance of  $8.50 \text{ \AA}$  in real space. Representative SEM images showing disordered platelets of PTI/Br (E, and F).

kinetics typical of protonated aromatic environments, which can be attributed to the bridging imide-bonds, unreacted end-groups or phase impurities (Fig. 2, B).

$^{15}\text{N}$  CP/MAS NMR data was referenced to glycine and shows three to four resonances similar to those reported for PTI/ $\text{Li}^+\text{Cl}^-$ .<sup>28</sup> The broad feature with principal maxima at 203.2 and 186.7 ppm is in the region of ternary nitrogen environments. The broad resonance at 131.9 ppm is a NH-environment as confirmed by dipolar dephasing experiments conducted by Schnick et al.<sup>28</sup> A weak shoulder at 142.9 ppm is assigned to a split of the NH-signal by  $\text{Li}^+/\text{H}^+$  disorder in the structure, but it can be assumed that most imide-bridges in PTI/Br have no lithium ions in their environment – which is in agreement with the deficiency of lithium in the elemental composition (Fig. 2, C).

Transmission electron microscopy (TEM) and selected area electron diffraction (SAED) confirm hexagonal symmetry of PTI/Br on molecular level with a lattice constant of  $8.50 \text{ \AA}$  in the

$hk0$  plane (Fig. 3, B, C, and D). The broad diffraction spots running diagonally across Fig. 3, B correspond to real space distances of  $3.52 \text{ \AA}$  for the inner spot and  $1.76 \text{ \AA}$  for the outer

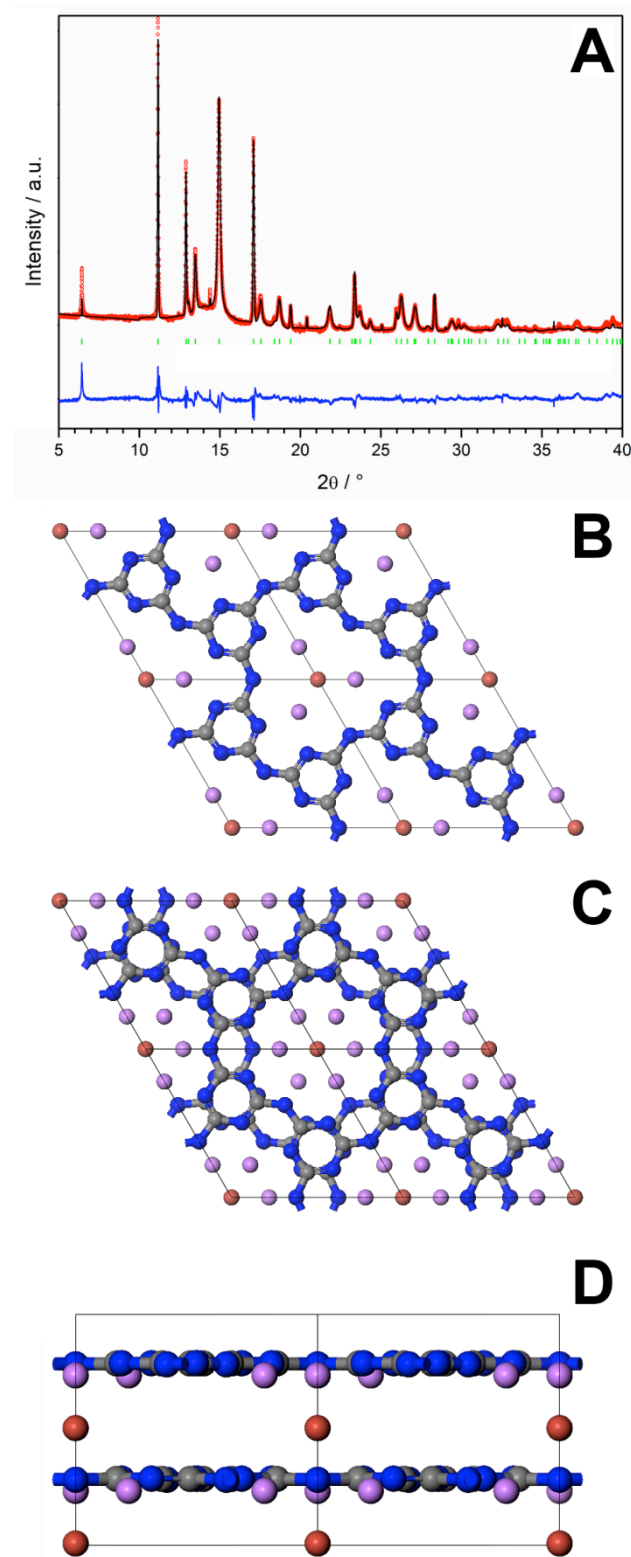


**Fig. 4** Rietveld refinement performed on the PXRD pattern of PTI/Br ( $R_{wp} = 2.20 \%$ ,  $R_p = 1.74 \%$ ,  $\chi^2 = 3.72$ ) with the observed pattern in black, refined profile in red, difference plot in blue, and Bragg peak positions in green (A). Projection along the  $c$ -axis of one layer (B) and two

consecutive layers (C) of PTI/Br with carbon, nitrogen, lithium and bromide atoms represented as grey, blue, purple and red spheres, respectively. Projection along the *b*-axis showing Br-anions in the interlayer space (D). The parameters of the hexagonal unit cell (*P*6<sub>3</sub>*cm*, no. 185) are *a* = 8.500390(68) Å, *c* = 7.04483(17) Å.

spot and can be assigned to expected reflexes (0 0 2) and (0 0 4), respectively, for a principal lattice constant *c* = 7.04 Å. Sharp reflexes in the *hk0* plane and diffuse diffraction along the *00l* direction suggest a high degree of in-plane order, but a level of turbostratic disorder in the stacking arrangement of individual layers. This is confirmed in the micro-scale make-up of PTI/Br from SEM images (Fig. 3, D, and E). Although sheets of the material are discernible, they do not seem to form ordered stacks as might be expected.

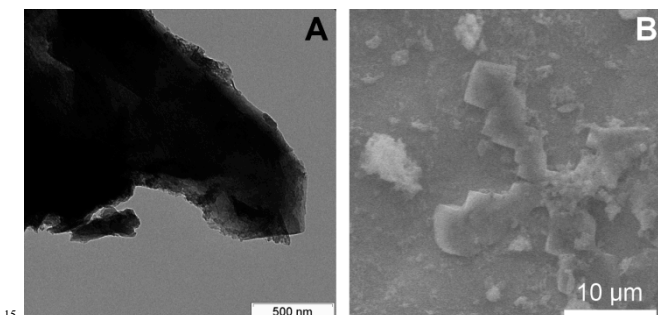


**Fig. 5** Representative TEM (A), and SEM image (B) of a PTI/F and PTI/Br phase-mix showing disordered platelets.

Rietveld refinement of the powder X-ray diffraction (PXRD) pattern of PTI/Br gave an atomic structure analogous to PTI/Li<sup>+</sup>Cl<sup>-</sup> and C<sub>6</sub>N<sub>9</sub>H<sub>3</sub>·HCl based on a 2D, planar arrangement of imide-linked triazine (C<sub>3</sub>N<sub>3</sub>) units (Fig. 4). The trigonal voids spanned by neighbouring triazine units are superimposed on top of each other, forming 1D pore channels which are decorated by the intercalated halides (Fig. 4, B, and C). Layers of the material are stacked in a graphitic, AB-fashion with the bromide anions situated in the interstitial space (Fig. 4, D). This leads to an expanded gallery height of 3.52 Å. The expansion of the stacking distance as compared to PTI/Li<sup>+</sup>Cl<sup>-</sup> can be rationalised taking the radii of the intercalated halide anions into consideration. Chlorine has a crystal radius of 1.67 and an ionic radius of 1.81 Å, while for bromine the values are 1.82 and 1.96 Å, respectively.<sup>32, 33</sup> Replacing Cl for Br in a layered PTI-structure would hence give an increase of the radius of the guest of 0.15 Å regardless of whether the electronic environment of the halide is more lattice crystalline or more ionic. This correlates closely with the actual increase of the gallery height of 0.14 Å, which corroborates that the halide anions must be (at least partially) situated in the interstitial space between layers.

Since the gallery height of PTI can be expanded with larger halide anions, decrease of stacking distance should be achievable with smaller anions. However, the use of a fluorine-based reaction medium or eutectic analogous to LiCl/KCl and LiBr/KBr for the ab initio synthesis of a PTI with intercalated fluoride ions is impractical and potentially dangerous due to the very likely formation of reactive fluoride-containing intermediates during the ionothermal condensation and the corrosive properties of fluorides towards glass in general. Partial intercalation of fluoride anions into PTI can be achieved however via post-synthetic

treatment of PTI/Br with concentrated ammonium fluoride (NH<sub>4</sub>F). Elemental microanalysis and ICP of the product gives a composition of C<sub>12</sub>N<sub>16.4</sub>H<sub>6.2</sub>Br<sub>0.09</sub>F<sub>1.73</sub>Li<sub>0.50</sub> (C, 32.2; N, 51.4; H, 1.39; O, 5.2; Br, 1.77; F, 7.32; and Li, 0.78 wt %), which hints at incomplete substitution. The micro-scale morphology of the

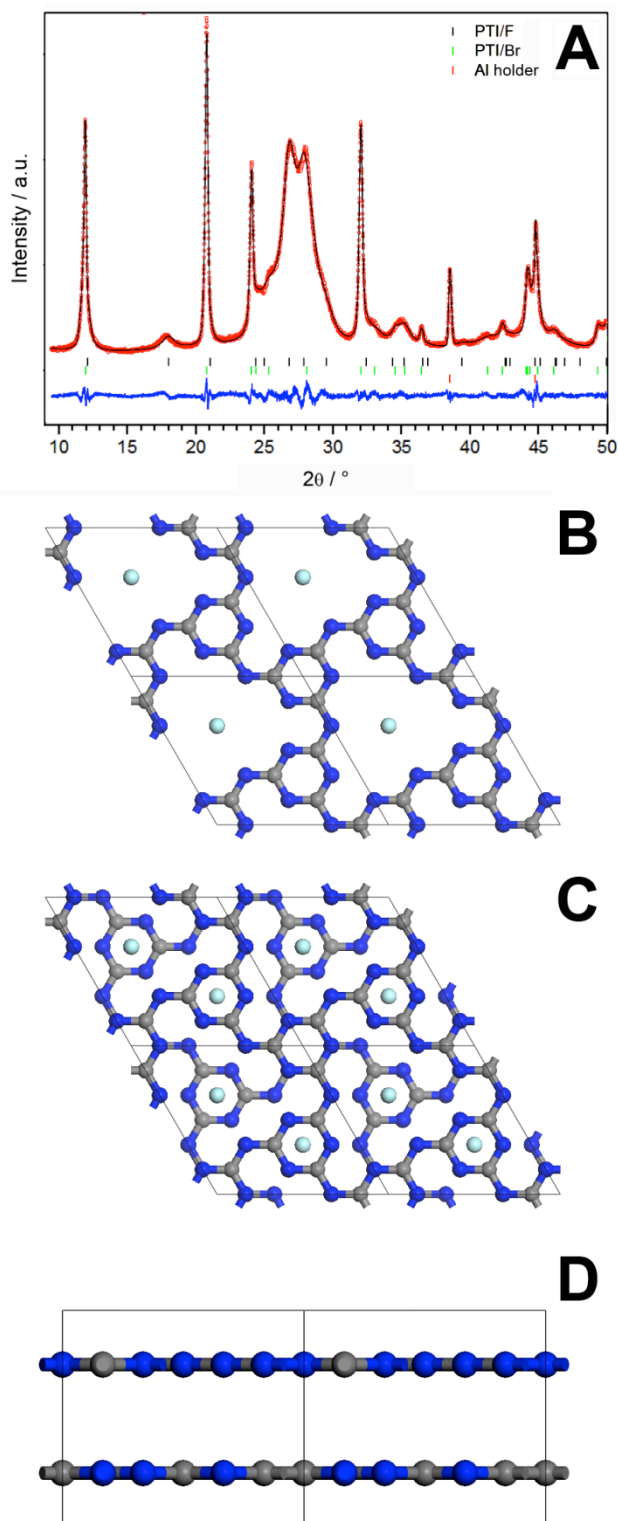


**Fig. 6** LeBail fit modelled as a two-phase mixture of PTI/F and PTI/Br with the observed pattern in black, fitted profile in red, and difference plot in blue (*R*<sub>wp</sub> = 3.89 %, *R*<sub>p</sub> = 3.05 %  $\chi^2$  = 1.42). Bragg peak positions are

shown as dashes in black for PTI/F, in green for PTI/Br and in red for the Al-sample holder, respectively (A). Projection along the *c*-axis of one layer (B) and two consecutive layers (C) of PTI/F with carbon, nitrogen, and fluoride atoms represented as grey, blue, purple and teal spheres, respectively. Projection along the *b*-axis. F-anions are situated within the void-space (D). The parameters of the hexagonal unit cell (*P*6<sub>3</sub>/*m*, no. 176) are *a* = 8.4212(4) Å, *c* = 6.6381(5) Å.

product has not been affected by the post-synthetic modification – disordered platelets are visible in TEM and SEM (Fig. 5).

The PXRD pattern of the recovered product is shown in Fig. 6, A. All peaks attributed to *hk0* reflexes for PTI/Br are present with (essentially) identical FWHM values, indicating that in-plane order has been retained. Reflexes with an *l* component however show a significant broadening. Furthermore, new, broad features appear at 17.9, 26.9, 29.5, and 50.0 ° (2θ, Cu Kα). These peaks can be rationalised assuming not only a different gallery height but also a different stacking arrangement. The broadness of reflexes with *l* components renders direct methods of structure solution from PXRD unfeasible. However, the proposed phase, PTI/F, can be constructed in structural analogy to C<sub>6</sub>N<sub>9</sub>H<sub>3</sub>·HCl, as it does not show the halide-containing 1D channels of PTI/Li<sup>+</sup>Cl<sup>-</sup> and PTI/Br. The layers of PTI/F stack in an AB-fashion – voids of layer A, however, lie on top of voids of subsequent layer B (Fig. 6, C). The gallery height of PTI/F has been decreased to 3.32 Å – a value smaller than that of graphite with a stacking distance of 3.35 Å. It is unclear from PXRD to which extent the substitution of bromide by fluoride anions has gone to completion, since the principle peak-positions in the observed PXRD pattern in Fig. 6, A can be rationalised as a phase-pure PTI/F with pronounced turbostratic disorder or as a mixture of PTI/F and PTI/Br (c.f. Bragg peak positions in Fig. 6, A). In the light of the results from elemental microanalysis, it is more probable to assume a mix of phases and a statistical substitution of guests in the PTI structure. Undoubtedly though, the interlayer distance of (at least a part) of the PTI material has been substantially decreased from 3.52 to 3.32 Å. This difference can be attributed to the size of the intercalated halides (F; crystal radius of 1.145 and ionic radius of 1.285 Å, Br; crystal radius of 1.82 and ionic radius of 1.96 Å, respectively). A fluoride anion is sufficiently small to find place within the trigonal cavities in the C, N plane (Fig. 6, B, and D). It does not protrude significantly into the inter-layer space and hence van der Waals interactions between the C, N planes determine the gallery height of PTI/F rather than steric repulsion exerted by the guest.

## Conclusions

The 2D, layered graphitic carbon nitride network – poly(triazine imide) (PTI) – has been obtained as an intercalation compound with the halides bromide (PTI/Br) and fluoride (PTI/F). The yellow-brownish materials both have hexagonal space groups (PTI/Br; *P*6<sub>3</sub>*cm*, no. 185 and PTI/F; *P*6<sub>3</sub>/*m*, no. 176) with parameters of *a* = 8.500390(68) Å, *c* = 7.04483(17) Å for PTI/Br and *a* = 8.4212(4) Å, *c* = 6.6381(5) Å for PTI/F, respectively, as established by Rietveld refinement, LeBail extraction and HRTEM studies, and are structurally related to PTI/L<sup>+</sup>Cl<sup>-</sup>, C<sub>6</sub>N<sub>9</sub>H<sub>3</sub>·HCl and other hypothetical graphitic phases of C<sub>3</sub>N<sub>4</sub>. On the basis of <sup>13</sup>C and <sup>15</sup>N NMR spectra it is confirmed that the

unit-cell of intercalated PTI contains two layers of imide-bridged triazine (C<sub>3</sub>N<sub>3</sub>) units stacked in an AB-fashion. Intriguingly, the gallery height of the layered PTI materials varies with the diameter of the intercalated host. In the series of crystal and ionic radii of halogens X = F < Cl < Br the PTI/X intercalation materials follow the same trend with stacking distances of 3.32, 3.38, and 3.52 Å for PTI/F, PTI/Cl and PTI/Br, respectively. Herein, PTI/F shows a gallery height smaller than that of graphite (3.35 Å), suggesting that the fluoride guest anion is situated in the large voids in the C, N plane, while chloride and bromide anions protrude into the interstitial space between the C, N planes and hence expand the gallery height according to their radii.

Most significantly, this work shows the relative ease with which tuning of the gallery height of hypothetically infinite, two-dimensional, covalently bonded molecular sheets can be achieved through intercalation of guests. The direct analogy of these C, N materials to the carbon-only layered system – graphite – is striking, and investigations into a potential pathway for the exfoliation of this interesting 2D material will be presented elsewhere.

## Acknowledgment

The authors thank EPSRC for funding (EP/H000925) and also EPSRC and E.ON for funding (EP/C511794/1) through the E.ON-EPSRC strategic call on CCS. A. I. C. is a Royal Society Wolfson Merit Award holder. The Max Planck Society is acknowledged for financial support within the EnerChem network. We thank Diamond Light Source for access to beamline I11 and Dr. Julia Parker for assistance during the experiment.

## Notes and references

<sup>a</sup> University of Liverpool, Department of Chemistry and Centre for Materials Discovery, Crown Street, Liverpool, L69 7ZD, UK. Tel: +447863699856; E-mail: m.j.bojdy.02@cantab.net

<sup>b</sup> School of Pharmacy, University of East Anglia, Norwich Research Park, Norwich, NR4 7TJ, UK.

<sup>c</sup> Technische Universität Berlin, Institut für Chemie, Sekr. C2, Hardenbergstrasse 40, 10623 Berlin, Germany.

<sup>d</sup> Max Planck Institute of Colloids and Interfaces, Research Campus Golm, 14424 Potsdam, Germany.

† Electronic Supplementary Information (ESI) available: Experimental (continued), Characterisation methods, <sup>1</sup>H-<sup>13</sup>C CP/MAS NMR kinetics data. See DOI: 10.1039/b000000x/

1. M. L. Cohen, *Phys. Rev. B, Condens. Matter*, 1985, **32**, 7988-7991.
2. A. Y. Liu and M. L. Cohen, *Science*, 1989, **245**, 841-842.
3. D. M. Teter and R. J. Hemley, *Science*, 1996, **271**, 53-55.
4. E. Kroke and M. Schwarz, *Coord. Chem. Rev.*, 2004, **248**, 493-532.
5. E. Horvath-Bordon, R. Riedel, P. F. McMillan, P. Kroll, G. Mieke, P. A. van Aken, A. Zerr, P. Hoppe, O. Shebanova, I. McLaren, S. Lauterbach, E. Kroke and R. Boehler, *Angew. Chem.-Int. Edit.*, 2007, **46**, 1476-1480.
6. A. Salamat, K. Woodhead, P. F. McMillan, R. Q. Cabrera, A. Rahman, D. Adriaens, F. Cora and J. P. Perrillat, *Phys. Rev. B*, 2009, **80**.
7. F. Goettmann, A. Fischer, M. Antonietti and A. Thomas, *Chem. Commun.*, 2006, 4530-4532.
8. F. Goettmann, A. Thomas and M. Antonietti, *Angew. Chem.-Int. Edit.*, 2007, **46**, 2717-2720.

- 
9. X. Wang, S. Blechert and M. Antonietti, *ACS Catalysis*, 2012, **2**, 1596-1606.
10. X. Wang, K. Maeda, A. Thomas, K. Takanebe, G. Xin, J. M. Carlsson, K. Domen and M. Antonietti, *Nat Mater*, 2009, **8**, 76-80.
11. M. Deifallah, P. F. McMillan and F. Cora, *J. Phys. Chem. C*, 2008, **112**, 5447-5453.
12. J. Sakamoto, J. van Heijst, O. Lukin and A. D. Schlüter, *Angew. Chem.-Int. Edit.*, 2009, **48**, 1030-1069.
13. J. C. Meyer, A. K. Geim, M. I. Katsnelson, K. S. Novoselov, T. J. Booth and S. Roth, *Nature*, 2007, **446**, 60-63.
14. A. K. Geim and K. S. Novoselov, *Nat. Mater.*, 2007, **6**, 183-191.
15. P. Kuhn, M. Antonietti and A. Thomas, *Angew. Chem.-Int. Edit.*, 2008, **47**, 3450-3453.
16. O. M. Yaghi, M. O'Keeffe, N. W. Ockwig, H. K. Chae, M. Eddaoudi and J. Kim, *Nature*, 2003, **423**, 705-714.
17. R. C. DeVries, *Mater. Res. Innov.*, 1997, **1**, 161-162.
18. P. H. Fang, *J. Mater. Sci. Lett.*, 1995, **14**, 536-538.
19. T. Malkow, *Mater. Sci. Eng. A-Struct. Mater. Prop. Microstruct. Process.*, 2000, **292**, 112-124.
20. S. Matsumoto, E. Q. Xie and F. Izumi, *Diam. Relat. Mat.*, 1999, **8**, 1175-1182.
21. W. Sundermeyer, *Angewandte Chemie*, 1965, **77**, 241-258.
22. W. Sundermeyer, *Chemie in unserer Zeit*, 1967, **1**, 150-157.
23. M. J. Bojdys, J. Jeromenok, A. Thomas and M. Antonietti, *Adv. Mater.*, 2010, **22**, 2202-2205.
24. M. J. Bojdys, S. A. Wohlgemuth, A. Thomas and M. Antonietti, *Macromolecules*, 2010, **43**, 6639-6645.
25. P. Kuhn, A. Forget, D. S. Su, A. Thomas and M. Antonietti, *J. Am. Chem. Soc.*, 2008, **130**, 13331-13337.
26. P. Kuhn, A. Thomas and M. Antonietti, *Macromolecules*, 2009, **42**, 319-326.
27. M. J. Bojdys, J.-O. Mueller, M. Antonietti and A. Thomas, *Chem.-Eur. J.*, 2008, **14**, 8177-8182.
28. E. Wirnhier, M. Döblinger, D. Gunzelmann, J. Senker, B. V. Lotsch and W. Schnick, *Chemistry – A European Journal*, 2011, **17**, 3213-3221.
29. J. George J., *Molten Salts Handbook*, Academic Press, London, 1967.
30. P. F. McMillan, V. Lees, E. Quirico, G. Montagnac, A. Sella, B. Reynard, P. Simon, E. Bailey, M. Deifallah and F. Cora, *J. Solid State Chem.*, 2009, **182**, 2670-2677.
31. Z. Zhang, K. Leinenweber, M. Bauer, L. A. J. Garvie, P. F. McMillan and G. H. Wolf, *J. Am. Chem. Soc.*, 2001, **123**, 7788-7796.
32. L. H. Ahrens, *Geochimica et Cosmochimica Acta*, 1952, **2**, 155-169.
33. L. Pauling, *The Nature of the Chemical Bond*, Cornell University Press, Ithaca, 1960.